JOURNAL OF AIRCRAFT
Vol. 42, No. 5, September–October 2005

Range Maximization for Emergency Landing After Engine Cutoff

Ilana Shapira* and Joseph Ben-Asher†
Technion—Israel Institute of Technology, 32000 Haifa, Israel

A pilot who experiences engine cutoff when flying at an envelope point of high velocity and low altitude needs as much range and altitude as possible for safe landing. An algorithm is presented that converts the velocity excess into altitude and range in an optimal way. Such an algorithm can be implemented after engine cutoff as the first stage of an emergency landing. The optimization problem is identified as a two-timescale problem composed of a short-duration initial boundary layer, followed by a long segment dominated by slow behavior. The slow segment represents the classical quasi-steady-state glide, whereas the boundary layer determines the fast dynamic phase in which the excess of the dynamic pressure is converted into the steady-state dynamic pressure while reaching the highest altitude. The boundary-layer section is solved by the dichotomic basis method and applied to the F-16, and the ensuing solution is compared to the exact one. The match between the two is very good.

Introduction

OPTIMAL energy conversion into range is of interest for airplanes if the engine fails because of fuel shortage or technical reasons, for gliders, or in planetary entry problems. For high-performance aircraft, the operational speeds have moved into the region where dynamic effects could no longer be neglected. As a result, the maximum range trajectory has boundary layers that drive the vehicle during the initial phase to the stabilized section and in the final phase from the stabilized section to the desired final state, in an optimal way.

The only rigorous method, which considers all dynamic effects, is the optimal control theory. However, the necessary conditions incorporated in this method appear in the form of a Hamiltonian two-point boundary-value problem. Such a problem can be solved numerically but with a substantial computational effort, due to hypersensitivity.[1–3] Hypersensitive problems are extremely sensitive to unknown boundary conditions that arise naturally in Hamiltonian problems. Thus, an approximated method should be used. The most common and natural approximation for a hypersensitive system is the singular perturbation theory (SPT), based on timescale separation. The concept of timescale separation stems from that different state variables change on different timescales so that the slow ones can be "on hold" while the fast ones converge to their stabilized values.

The problem focuses on the vertical plane, where the state variables are range, altitude, velocity, and path angle, and the lift coefficient is the control. Ardema and Rajan[4] listed the timescale assumptions used or proposed in past (before 1985) analyses of aircraft trajectory optimization by the SPT. In all papers that dealt with vertical or three-dimensional flight, the path angle was chosen as the fastest variable, with altitude being comparable or slower. In all cases, the velocity was replaced by the energy, which was always slower than the altitude. The last assumption complies with the energy conservation law for a nondissipative system. If a vehicle experiences comparable drag and thrust forces, the same approximation may still hold. However, for airplanes, which are under drag force with no canceling thrust, the approximation is questionable. In Refs. 5 and 6, the same maximum range problem was treated with timescale separation based on three-timescale separation: The velocity and path angle were assumed to be faster than the altitude and range, and the path angle was assumed to be faster than the velocity. Such a separation produces a main boundary layer that keeps the altitude on hold while considering the dynamic fast change of the velocity and path angle. The main boundary layer has an internal sublayer that keeps the velocity on hold, changing the path angle first. This formulation defines boundary layers such that each one has only one active variable, thus, enabling an analytical solution of the boundary layers that produces an open-loop solution of the trajectory and a feedback law for the control. The ensuing solutions were compared to the exact ones, and the matching between the approximated solutions and the exact numerical solutions were studied. The open-loop solutions showed good agreement for those cases where the initial dynamic pressure was much higher than the stabilized one. The feedback solutions were reasonable except for induced oscillations that appeared when the boundary layer intercepted the steady-state segment. The oscillations result because the path-angle time constant is not faster than that of the velocity when approaching the stabilized section.

In this paper, the same maximum range problem is treated, but as a two-time-constant problem instead of a three-time-constant problem. The path angle and the velocity time constants are considered comparable, but faster than the altitude and range. Under this assumption, numerical solutions based on the dichotomic basis method[1] are derived. The dichotomic basis approach's objective is to develop an indirect solution method for nonlinear two-timescale optimal control problems, a solution method based on underlying geometric structure of the trajectories of the Hamiltonian system but not requiring a priori knowledge of this structure. Two capabilities are required: splitting the Hamiltonian system into slow and fast parts and splitting the fast part into contracting and expanding parts. The expanding part is suppressed in the initial boundary layer, thus, enabling an easier convergence of the solution.

Model Description

The airplane is represented by a point mass in a fixed and flat Earth. The model is described by four equations of motion (no thrusting forces):

$$\frac{\mathrm{d}x}{\mathrm{d}t} = v \cdot \cos(\gamma) \tag{1a}$$

$$\frac{\mathrm{d}h}{\mathrm{d}t} = v \cdot \sin(\gamma) \tag{1b}$$

$$\frac{\mathrm{d}v}{\mathrm{d}t} = -\frac{D}{m} - g \cdot \sin(\gamma) \tag{1c}$$

$$\frac{\mathrm{d}\gamma}{\mathrm{d}t} = \left(\frac{L}{w} - \cos(\gamma)\right) \cdot \frac{g}{v} \tag{1d}$$

Received 12 April 2004; revision received 20 June 2004; accepted for publication 21 June 2004.

*Graduate Student, Faculty of Aeronautical Engineering; ishapira@bezeqint.net.

†Associate Professor, Faculty of Aeronautical Engineering, Technion. Associate Fellow AIAA.

where

$$D = cd \cdot q \cdot s, \qquad L = cl \cdot q \cdot s, \qquad q = 0.5 \cdot \rho \cdot v^2$$

The parabolic drag and exponential atmosphere models are assumed:

$$cd = cd_0 + k \cdot cl^2, \qquad \rho(h) = \rho_{sl} \cdot \exp[-(h/h_{\text{ref}})]$$

Problem Formulation

The framework of the optimization is that of optimal control where the cost is the final range $x(t_f)$ and the control is the lift coefficient cl. The initial boundary conditions are h_0, v_0, and γ_0, and the terminal boundary conditions are h_f, v_f, and γ_f.

The two-timescale problem of the boundary-layer type has a generic solution that is composed of a short-duration initial boundary-layer segment dominated by fast contracting behavior, a long-duration intermediate segment dominated by slow behavior, and a short-duration terminal boundary-layer segment dominated by fast expanding behavior.

The steady-state intermediate segment is solved in the traditional way as the reduced segment of the SPT problem, and the boundary segments are solved by using a dichotomic basis[1] and eliminating the unstable components of the Hamiltonian vector field. The elimination of the unstable components removes the hypersensitivity and simplifies the numerical convergence of the solution. Concatenating the three-segments solution approximates the solution of the complete problem. Because the initial boundary-layer solution is an analog to the terminal one, only the initial boundary layer is solved in this paper.

The state equations in the SPT approximation for a two-time-constant system are given as

$$\frac{\mathrm{d}x}{\mathrm{d}t} = v \cdot \cos(\gamma) \tag{2a}$$

$$\frac{\mathrm{d}h}{\mathrm{d}t} = v \cdot \sin(\gamma) \tag{2b}$$

$$\varepsilon \cdot \frac{\mathrm{d}v}{\mathrm{d}t} = -\frac{D}{m} - g \cdot \sin(\gamma) \tag{2c}$$

$$\varepsilon \cdot \frac{\mathrm{d}\gamma}{\mathrm{d}t} = \left[\frac{L}{w} - \cos(\gamma)\right] \cdot \frac{g}{v} \tag{2d}$$

The cost function is $J = -x_f$, and the Hamiltonian becomes

$$H = \lambda_x \cdot v \cdot \cos(\gamma) + \lambda_h \cdot v \cdot \sin(\gamma) + \lambda_v \cdot [-D/m - g \cdot \sin(\gamma)] + \lambda_\gamma \cdot [L/w - \cos(\gamma)] \cdot g/v \tag{3}$$

It is convenient to decompose the Hamiltonian into two components to be used in the different layers:

$$H^0 = \lambda_x \cdot v \cdot \cos(\gamma) + \lambda_h \cdot v \cdot \sin(\gamma) \tag{4a}$$

$$H^1 = \lambda_v \cdot [-D/m - g \cdot \sin(\gamma)] + \lambda_\gamma \cdot [L/w - \cos(\gamma)] \cdot g/v \tag{4b}$$

The costates satisfy the Euler–Lagrange equations:

$$\frac{\mathrm{d}\lambda_x}{\mathrm{d}t} = -\frac{\partial H}{\partial x} = 0 \tag{5a}$$

$$\frac{\mathrm{d}\lambda_h}{\mathrm{d}t} = -\frac{\partial H}{\partial h} = -\frac{s}{2m} \cdot \frac{\rho}{h_{\text{ref}}}\left(\lambda_v \cdot cd \cdot v^2 - \lambda_\gamma \cdot cl \cdot v\right) \tag{5b}$$

$$\varepsilon \cdot \frac{\mathrm{d}\lambda_v}{\mathrm{d}t} = -\frac{\partial H}{\partial v} = -\left\{\lambda_x \cdot \cos(\gamma) + \lambda_h \cdot \sin(\gamma) - \frac{\lambda_v}{m} \cdot \frac{\partial D}{\partial v} + \lambda_\gamma \cdot \frac{\partial}{\partial v}\left[\frac{L}{w} - \cos(\gamma)\right] \cdot \frac{g}{v}\right\} \tag{5c}$$

$$\varepsilon \cdot \frac{\mathrm{d}\lambda_\gamma}{\mathrm{d}t} = -\frac{\partial H}{\partial \gamma} = -\left[-\lambda_x \cdot v \cdot \sin(\gamma) + \lambda_h \cdot v \cdot \cos(\gamma) - \lambda_v \cdot g \cdot \cos(\gamma) + \frac{\lambda_\gamma \cdot g}{v}\sin(\gamma)\right] \tag{5d}$$

The initial and final values of the states and costates of the full problem are

$$x(0) = 0, \qquad x(t_f) \text{ free}, \qquad \lambda_x = -1 \tag{6a}$$

$$h(0) = h_0, \qquad h(t_f) = h_f, \qquad \lambda_h(t_f) \text{ unknown} \tag{6b}$$

$$v(0) = v_0, \qquad v(t_f) = v_f, \qquad \lambda_v(t_f) \text{ unknown} \tag{6c}$$

$$\gamma(0) = \gamma_0, \qquad \gamma(t_f) = \gamma_f, \qquad \lambda_\gamma(t_f) \text{ unknown} \tag{6d}$$

Outer (Slow) Solution

The outer solution was derived in Ref. 5, and is given in Appendix A. It is shown that γ, q, and cl in the outer section (denoted by γ^o, q^o, cl^o) are given by

$$\tan(\gamma^o) = -2\sqrt{cd_0 \cdot k} \tag{7a}$$

$$q^o = (w/s)\sqrt{k/cd_0} \cdot 1\Big/\sqrt{1 + 4 \cdot cd_0 \cdot k} \tag{7b}$$

$$cl^o = \sqrt{cd_0/k} \tag{7c}$$

The Lagrange coefficient λ_h is constant given by

$$\lambda_h = -1\Big/2\sqrt{cd_0 \cdot k} \tag{7d}$$

The outer lift coefficient is the classical well-known coefficient for a steady-state optimal glide. This justifies our assumptions for the outer approximation, which represents the steady-state section of the flight.

The slow states x, h, and v change in time according to

$$x^o(t) = -2h_0\Big/\tan(\gamma^o) \cdot \log\left(1 - v_0^o \cdot \beta \cdot t\right) \tag{8a}$$

The velocity v_0^o is the initial outer velocity defined by $\frac{1}{2} \cdot \rho(h_0) \cdot v_0^{o^2} = q^o$, or

$$v_0^{o^2} = 2 \cdot \exp(h_0/h_{\text{ref}})/\rho_{sl} \cdot (w/s)\sqrt{k/cd_0} \cdot 1\Big/\sqrt{1 + 4 \cdot cd_0 \cdot k}$$

$$\beta = \sin(\gamma^o)\Big/2h_0 \tag{8b}$$

$$h^o(t) = h_0 \cdot \left[1 - 2 \cdot \log\left(1 - v_0^o \cdot \beta \cdot t\right)\right] \tag{8c}$$

$$v^o(t) = v_0^o\Big/\left(1 - v_0^o \cdot \beta \cdot t\right) \tag{8d}$$

The state variables λ_v and λ_γ are given by

$$\lambda_v^o(t) = -\frac{v^o(t)}{2 \cdot g \cdot \sqrt{cd_0 \cdot k}} \tag{8e}$$

$$\lambda_\gamma^o(t) = -\frac{[v^o(t)]^2}{g} \tag{8f}$$

Initial (Fast) Boundary-Layer Formulation

The initial boundary layer is derived by changing the timescale from t to $\tau = t/\varepsilon$ and then substituting $\varepsilon = 0$ into the general formalism. All of the variables in the initial boundary layer are labeled with superscript i, which denotes the pertinence to the initial boundary layer. Also, the slow variables h and x are constant and equal to their initial values.

The velocity and path angle change according to

$$\frac{\mathrm{d}v^i}{\mathrm{d}\tau} = -\frac{D^i}{m} - g \cdot \sin(\gamma^i) \tag{9a}$$

$$\frac{\mathrm{d}\gamma^i}{\mathrm{d}\tau} = \left[\frac{L^i}{w} - \cos(\gamma^i)\right] \cdot \frac{g}{v^i} \tag{9b}$$

The boundary conditions of the state variables include the original initial conditions and final conditions that coincide with the initial outer values:

$$v^i(0) = v_0, \qquad v^i(\tau)|_{\tau\to\infty} = v_0^o \tag{10a}$$

$$\gamma^i(0) = \gamma_0, \qquad \gamma^i(\tau)|_{\tau\to\infty} = \gamma^o \tag{10b}$$

The initial Lagrange coefficients are not known, but their final values should coincide with the initial outer values:

$$\lambda_v^i(\tau)\big|_{\tau\to\infty} = \lambda_v^o(0) = -v_0^o\big/\left(2\cdot g\cdot\sqrt{cd_0\cdot k}\right) \tag{10c}$$

$$\lambda_\gamma^i(\tau)\big|_{\tau\to\infty} = \lambda_\gamma^o(0) = -\left[v_0^o\right]^2\big/g \tag{10d}$$

The cost function is redefined to compensate for freezing the slow variables x and h,

$$J = \lim_{\tau_f\to\infty}\int_0^{\tau_f} H^o\left[\lambda_x, \lambda_h, v^i(\tau), \gamma^i(\tau)\right]\mathrm{d}\tau \tag{11}$$

Thus, the original Hamiltonian of the initial layer H^i becomes

$$\begin{aligned} H^i &= H^o\left(\lambda_x, \lambda_h, v^i, \gamma^i\right) \\ &\quad + H^1\left[\lambda_v, D\left(h_0, v^i, \gamma^i, cl^i\right), L\left(h_0, v^i, \gamma^i, cl^i\right), \gamma^i\right] \end{aligned}$$

or

$$\begin{aligned} H^i &= \lambda_x \cdot v^i \cdot \cos(\gamma^i) + \lambda_h \cdot v^i \cdot \sin(\gamma^i) \\ &\quad + \lambda_v^i \cdot \left[-D\left(h_0, v^i, \gamma^i, cl^i\right)\big/m - g\cdot\sin(\gamma^i)\right] \\ &\quad + \lambda_\gamma^i \cdot \left[(L/w)\left(h_0, v^i, \gamma^i, cl^i\right) - \cos(\gamma^i)\right]\cdot g/v^i = 0 \end{aligned} \tag{12}$$

The costate equations of λ_v^i and λ_γ^i are

$$\frac{\mathrm{d}\lambda_v^i}{\mathrm{d}\tau} = -\frac{\partial H}{\partial v^i} = -\left[\lambda_x\cdot\cos(\gamma^i) + \lambda_h\cdot\sin(\gamma^i) - \frac{\lambda_v^i}{m}\cdot\frac{\partial D\left(h_0, v^i\right)}{\partial v^i}\right] \tag{13}$$

$$\begin{aligned} \frac{\mathrm{d}\lambda_\gamma^i}{\mathrm{d}\tau} &= -\frac{\partial H}{\partial \gamma^i} = -\Bigg[-\lambda_x\cdot v^i\cdot\sin(\gamma^i) + \lambda_h\cdot v\cdot\cos(\gamma^i) \\ &\quad - \frac{\lambda_v^i}{m}\cdot\frac{\partial D\left(h_0, v^i, \gamma^i\right)}{\partial\gamma^i} - \lambda_v^i\cdot g\cdot\cos(\gamma^i)\Bigg] \end{aligned} \tag{14}$$

The zeroth-order inner formulation is given in Appendix B.

Dichotomic Basis Method

Dichotomic Basis

Equations (9–14) define a nonlinear Hamiltonian vector field $\bar{p}$ in the state–costate space

$$\boldsymbol{p} = (\boldsymbol{x}, \lambda)', \qquad \boldsymbol{x} = (\boldsymbol{v}, \gamma)', \qquad \lambda = (\lambda_v, \lambda_\gamma)' \tag{15}$$

$$\dot{\boldsymbol{p}} = \begin{bmatrix}\dot{\boldsymbol{x}}\\ \dot{\lambda}\end{bmatrix} = \begin{bmatrix} H_\lambda^T(\boldsymbol{x}, \lambda)\\ -H_x^T(\boldsymbol{x}, \lambda)\end{bmatrix} = G(\boldsymbol{p}) \tag{16}$$

The Hamiltonian first-order partial derivatives in the initial layer appear in Appendix C. The dichotomic basis[1–3] of this system splits this fast part into stable and unstable parts in the neighborhood of the equilibrium point, which is represented by the initial point of the outer solution. When the fast dynamics are linear, eigenvalues and eigenvectors can be used to split the stable and unstable parts. A dichotomic transformation serves the same purpose for nonlinear Hamiltonian boundary-value problem systems by decomposing the nonlinear vector field into its contracting and expanding components, thus, allowing the missing boundary conditions required to specify the boundary segments to be determined from partial equilibrium conditions. The key feature of the method is that, by using a dichotomic basis, the unstable (expanding) component of the Hamiltonian vector field can be eliminated, thereby, removing the hypersensitivity. The dichotomic basis $D(\boldsymbol{p})$ transforms $G(P)$ into linear flow $\boldsymbol{v}$ according to

$$G(\boldsymbol{p}) = D(\boldsymbol{p})\boldsymbol{v} \tag{17}$$

where $\boldsymbol{v}\in\mathbb{R}^{2n}$ are the components of $G(\boldsymbol{p})$ in the basis $D(\boldsymbol{p})$,

$$\dot{\boldsymbol{v}} = \Lambda\boldsymbol{v} \equiv \left[D^{-1}\frac{\partial G}{\partial \boldsymbol{p}}D - D^{-1}\dot{D}\right]\boldsymbol{v} \tag{18}$$

Columns of the matrix $D(\boldsymbol{p})$ form a dichotomic basis if $\Lambda(\boldsymbol{p})$ has the block-triangular form,

$$\Lambda(\boldsymbol{p}) = \begin{bmatrix}\Lambda_s(\boldsymbol{p}) & \Lambda_{su}(\boldsymbol{p})\\ 0 & \Lambda_u(\boldsymbol{p})\end{bmatrix}$$

(which expresses the decoupling the components of $\bar{v}$) and if the transition matrix of $\Lambda_s(\boldsymbol{p})$ contracts vectors exponentially in forward time, whereas the transition matrix of $\Lambda_u(\boldsymbol{p})$ contracts vectors exponentially in backward time.

If the matrix D is expressed as

$$D = \begin{bmatrix}\boldsymbol{I} & 0\\ P & \boldsymbol{I}\end{bmatrix}$$

then $\Lambda(\boldsymbol{p})$ takes the form

$$\Lambda(\boldsymbol{p}) = \begin{bmatrix}H_{\lambda x} + H_{\lambda\lambda}\boldsymbol{P} & H_{\lambda\lambda}\\ 0 & -H_{x\lambda} - PH_{\lambda\lambda}\end{bmatrix} \tag{19}$$

The Hamiltonian second order partial derivatives in the initial layer appear in Appendix D. The block-triangular form of $\Lambda(\boldsymbol{p})$ requires the fulfillment of the following Ricatti equation:

$$\dot{P} = -PH_{\lambda x} - H_{x\lambda}P - PH_{\lambda\lambda}P - H_{xx} \tag{20}$$

Also, because the solution in forward time lies in the stable manifold of $\bar{\boldsymbol{p}}$, then $\bar{P}\triangleq P(\tau)_{\tau\to\infty}$ should satisfy the algebraic equation

$$-\bar{P}H_{\bar{\lambda}\bar{x}} - H_{\bar{x}\bar{\lambda}}\bar{P} - \bar{P}H_{\bar{\lambda}\bar{\lambda}}\bar{P} - H_{\bar{x}\bar{x}} = 0 \tag{21}$$

Ricatti matrix P in steady state appear in Appendix E. The components of the linear time-varying vector $\boldsymbol{v}$ are denoted by $(h_s, h_u)'$

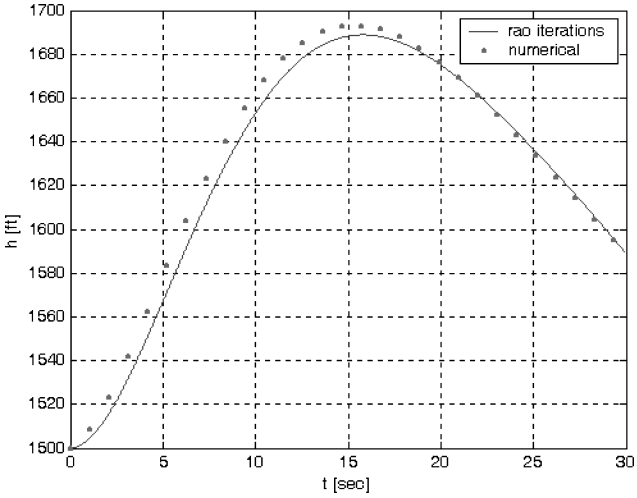

Fig. 1 Altitude vs time for initial velocity of 300 ft/s.

and if substituted in Eq. (17) and (18), they obey the following equations:

$$\dot{\boldsymbol{p}} = \begin{bmatrix} \dot{\boldsymbol{x}} \\ \dot{\lambda} \end{bmatrix} = \begin{bmatrix} H_{\lambda}^{T}(\boldsymbol{x}, \lambda) \\ -H_{x}^{T}(\boldsymbol{x}, \lambda) \end{bmatrix} = G(\boldsymbol{p}) = \begin{bmatrix} \boldsymbol{I} & 0 \\ P & \boldsymbol{I} \end{bmatrix} \begin{bmatrix} h_s \\ h_u \end{bmatrix} \quad (22)$$

$$\begin{bmatrix} \dot{h}_s \\ \dot{h}_u \end{bmatrix} = \begin{bmatrix} H_{\lambda x} + H_{\lambda\lambda} P & H_{\lambda\lambda} \\ 0 & -H_{x\lambda} - P H_{\lambda\lambda} \end{bmatrix} \begin{bmatrix} h_s \\ h_u \end{bmatrix} \quad (23)$$

Riccati Dichotomic Basis Method

The solution in the initial inner layer lies in the stable manifold of $\bar{p}$. Because this solution is decoupled from the unstable one, then if the unstable component h_u is set to zero at $t = 0$, it will stay zero. This condition is equivalent to the algebraic equations

$$[-P(0) \quad I] \begin{bmatrix} H_{\lambda} \\ -H_{x} \end{bmatrix} = 0 \quad (24)$$

From this set of equations, $\lambda_v(0)$ and $\lambda_\gamma(0)$ can be derived (Appendix F).

Once $\lambda_v(0)$ and $\lambda_\gamma(0)$ were solved, $h_s(0)$ can be derived from Eq. (22),

$$h_s(0) = H_{\lambda}(x_0, \lambda_0) = H_{\lambda}[v_0, \gamma_0, \lambda_v(0), \lambda_\gamma(0)] \quad (25)$$

or

$$h_s(0) = \begin{bmatrix} H_{\lambda_v}(0) \\ H_{\lambda_\gamma}(0) \end{bmatrix} = \begin{bmatrix} \left[-\dfrac{c d_0 \cdot \rho(h_0) \cdot s}{2 \cdot m} \right] \cdot v_0^2 - \left[\dfrac{\rho(h_0) \cdot s}{8 \cdot k \cdot m} \right] \cdot \dfrac{\lambda_\gamma(0)^2}{\lambda_v(0)^2} - g \cdot \sin(\gamma_0) \\ \left[\dfrac{\rho(h_0) \cdot s}{4 \cdot k \cdot m} \right] \cdot \dfrac{\lambda_\gamma(0)}{\lambda_v(0)} - g \cdot \dfrac{\cos(\gamma_0)}{v_0} \end{bmatrix} \quad (26)$$

Now with $h_u(0) \equiv 0$, the relevant system of differential equations from Eqs. (22) and (23) can be written more compactly as

$$\begin{bmatrix} \dot{\boldsymbol{x}} \\ \dot{\lambda} \\ \dot{h}_s \end{bmatrix} = \begin{bmatrix} \boldsymbol{I} \\ P \\ H_{\lambda x} + H_{\lambda\lambda} P \end{bmatrix} h_s \quad (27)$$

The initial conditions of $(\boldsymbol{x}, \lambda, h_s)$ are all known. The only unknown variable needed to integrate the system is the Riccati matrix $P(t)$.

Algorithm 1 in Ref. 1 suggests a successive approximation procedure for solving Eq. (27) in the initial boundary layer. It is based on choosing the convergence time of the initial layer to the steady-state

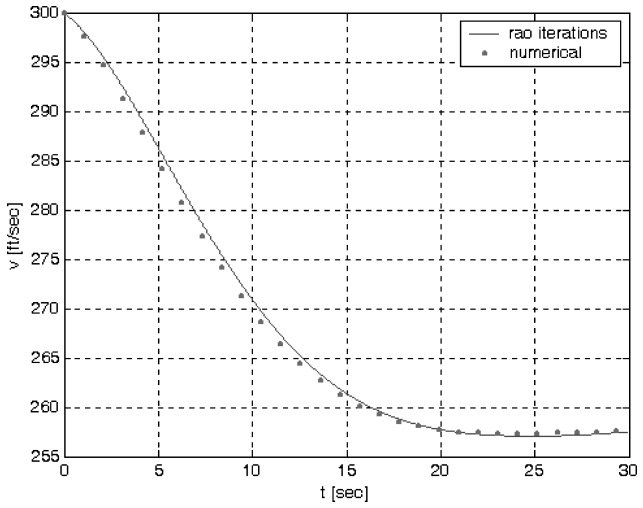

Fig. 2 Velocity vs time for initial velocity of 300 ft/s.

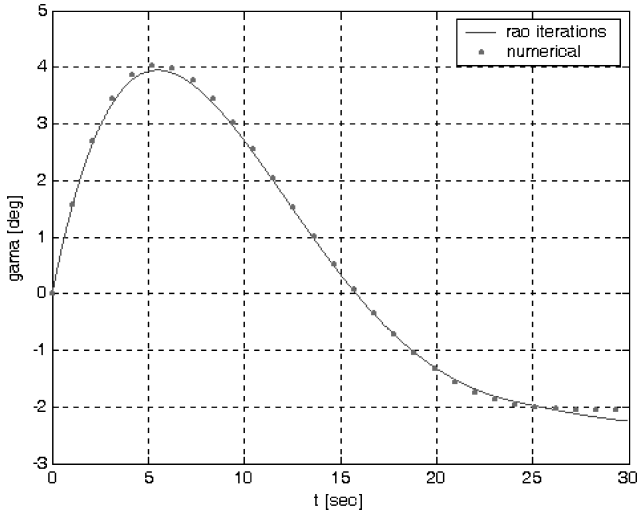

Fig. 3 Path angle vs time for initial velocity of 300 ft/s.

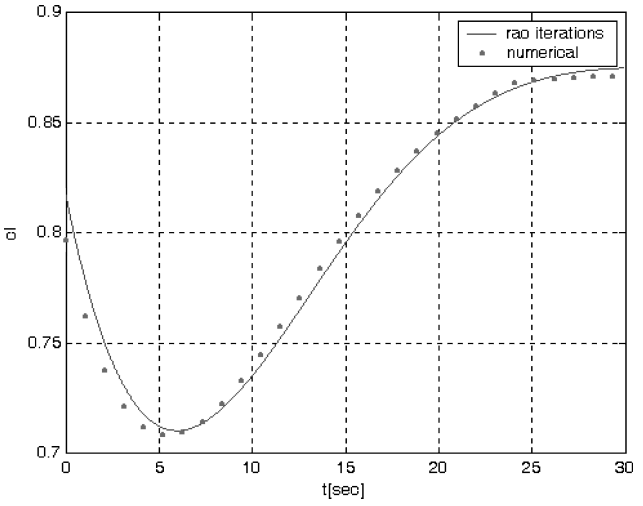

Fig. 4 Control vs time for initial velocity of 300 ft/s.

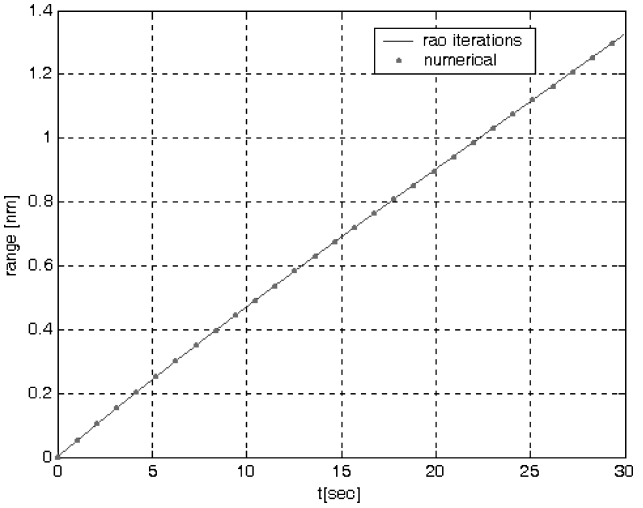

Fig. 5 Range vs time for initial velocity of 300 ft/s.

section t_{ibl}, and an initial guess of $P(t)$ that satisfies the steady-state known value. Then the differential equations (27) can be integrated from $t=0$ to $t=t_{\text{ibl}}$. Obviously, the final values of the state variables $\boldsymbol{x}(t_{\text{ibl}})=[v(t_{\text{ibl}}),\gamma(t_{\text{ibl}})]'$ would not equal their steady-state values from Eqs. (7a) and (8b), unless $P(t)$ is the correct Ricatti matrix. Therefore, the next step is to use $h_s(t)$ produced in the forward integration to carry out a backward integration of Eq. (27) from $t=t_{\text{ibl}}$ to $t=0$ of $\boldsymbol{p}=(\boldsymbol{x},\lambda)'$,

$$\begin{bmatrix}\dot{\boldsymbol{x}}\\ \dot{\lambda}\end{bmatrix}=\begin{bmatrix}\boldsymbol{I}\\ P\end{bmatrix}h_s \tag{28}$$

together with the differential equation of $P(t)$ given in Eq. (20). $P(t)$ is initiated by its equilibrium value derived from Eq. (21), and the other variables are initiated by their terminal conditions defined as the outer values of (x,λ). The outer values as a function of time are given in Eqs. (7a), (7d), (8b), and (8d–8f), and their values for t_{ibl} that should be used are $\tan(\gamma^o)=-2\sqrt{(cd_0\cdot k)}$ and

$$v^o(t_{\text{ibl}})=\frac{v_0^o}{1-v_0^o\cdot\sin(\gamma^o)\big/2h_0\cdot t_{\text{ibl}}} \tag{29}$$

$$v_0^{o^2}=2\cdot\frac{\exp(h_0/h_{\text{ref}})}{\rho_{sl}}\cdot\frac{w}{s}\sqrt{\frac{k}{cd_0}}\cdot\frac{1}{\sqrt{1+4\cdot cd_0\cdot k}} \tag{30}$$

$$\lambda_v^o(t_{\text{ibl}})=-\frac{v^o(t_{\text{ibl}})}{2\cdot g\cdot\sqrt{cd_0\cdot k}},\qquad \lambda_\gamma^o(t_{\text{ibl}})=-\frac{\left[v^o(t_{\text{ibl}})\right]^2}{g} \tag{31}$$

The backward integration updates the initial guess of $P(t)$ and enables the second iteration of the forward integration with the updated $P(t)$. This process continues until the final values of the forward integration converge to the outer values. If the iteration process on $P(t)$ does not converge, then the chosen time t_{ibl} should be increased.

Application of Method to Range Optimization for F-16

The Riccati dichotomic basis method is now applied to an F-16 flying at 1500 ft (457.2 m) and suffering from engine cutoff. The range optimization algorithm will transfer the excess velocity into an altitude from which the glide stage will carry the aircraft as far as possible, thereby giving the pilot enough time/range to plan a safe emergency landing.

The aircraft is represented by its four characteristics: weight of 8853 kg (19,543 lb), wing surface of 28 m^2 (301 ft^2), and drag parameters $cd_0=0.015$ and $k=0.02$. Actually, the weight and surface area amount to one parameter, that is, the load factor $w/s=316$ kg/m^2, ($w/s=65$ lb/ft^2), so that the aircraft is actually represented by three characteristics.

The iteration method described earlier was applied to the aircraft with different initial velocities and zero initial path angle. For the first low initial velocity of 300 ft/s, the initial guess for $P(t)$ was the equilibrium matrix, and for higher velocities the

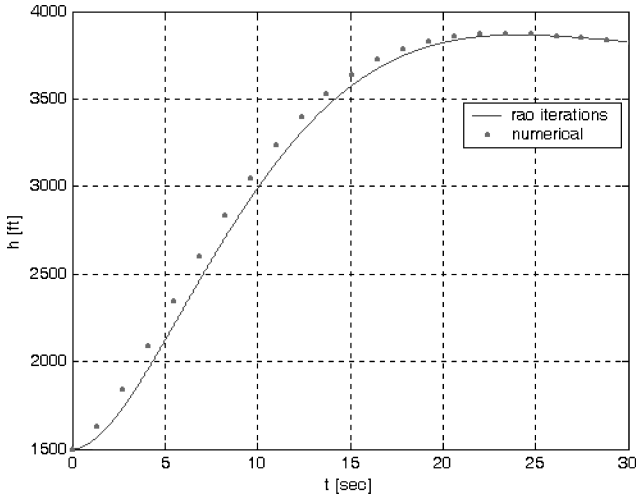

Fig. 6 Altitude vs time for initial velocity of 500 ft/s.

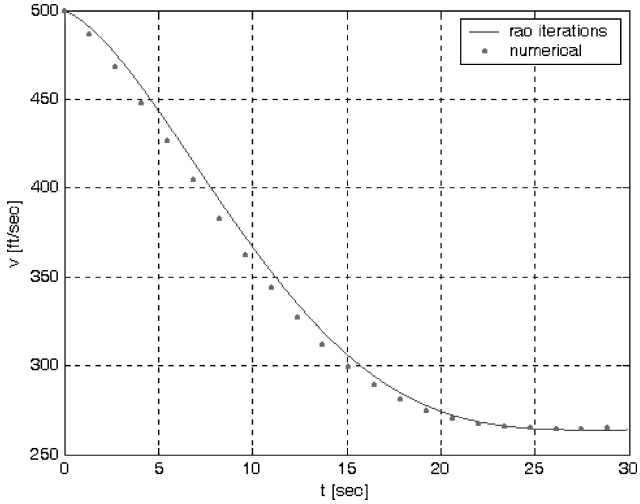

Fig. 7 Velocity vs time for initial velocity of 500 ft/s.

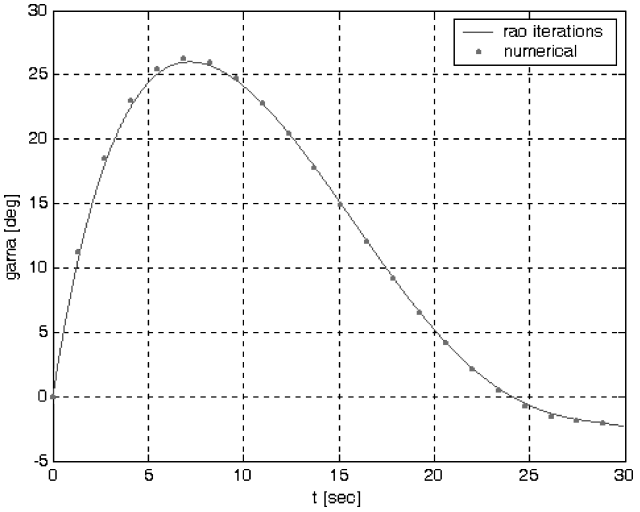

Fig. 8 Path angle vs time for initial velocity of 500 ft/s.

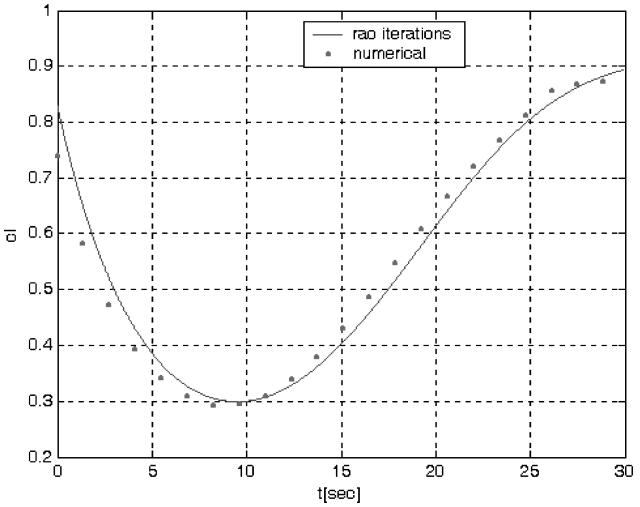

Fig. 9 Control vs time for initial velocity of 500 ft/s.

former solution served as the initial guess. The iteration process was stopped when the difference between the forward and backward trajectories was less than determined. The variables at convergence for initial velocities of 300 and 800 ft/s are given in Appendix G.

The initial boundary results of the inner variables of F-16, for initial velocities of 300, 500, and 800 ft/s, by Rao's iteration process vs numerical data are given in Figs. 1–15.

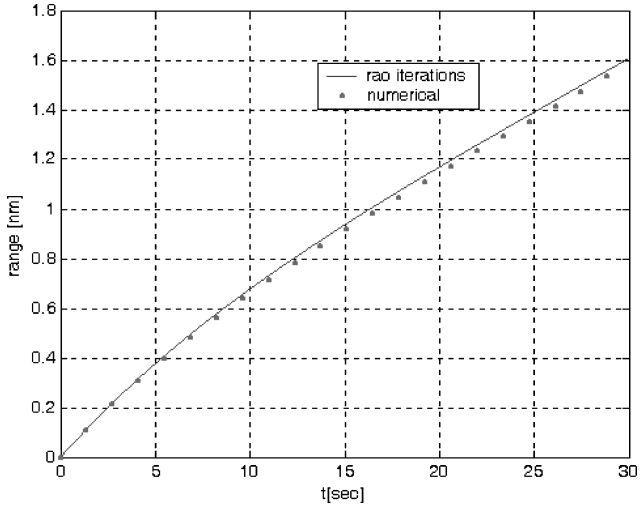

Fig. 10 Range vs time for initial velocity of 500 ft/s.

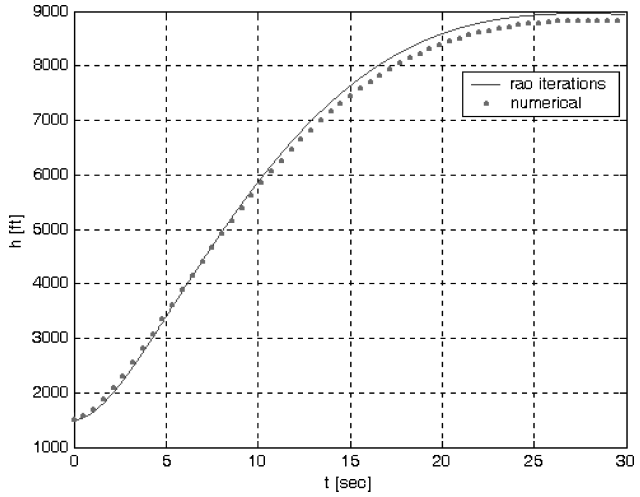

Fig. 11 Altitude vs time for initial velocity of 800 ft/s.

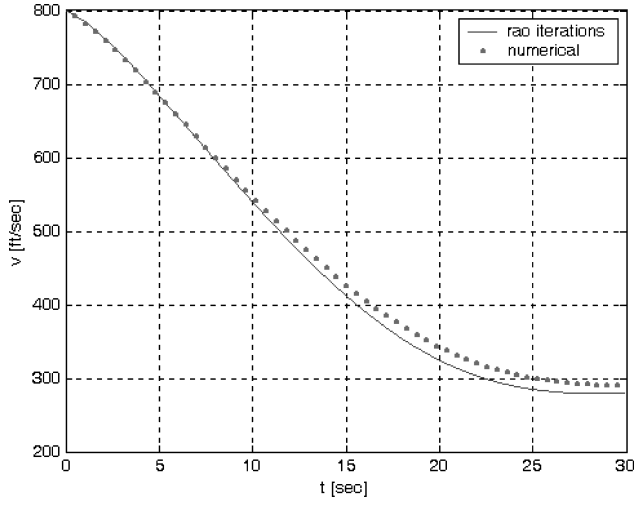

Fig. 12 Velocity vs time for initial velocity of 800 ft/s.

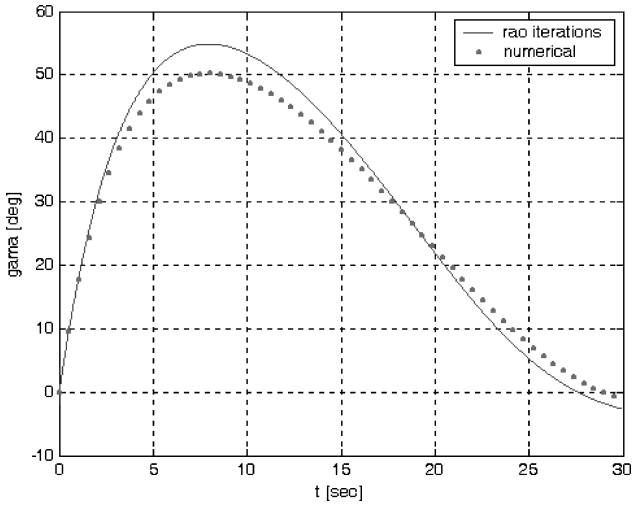

Fig. 13 Path angle vs time for initial velocity of 800 ft/s.

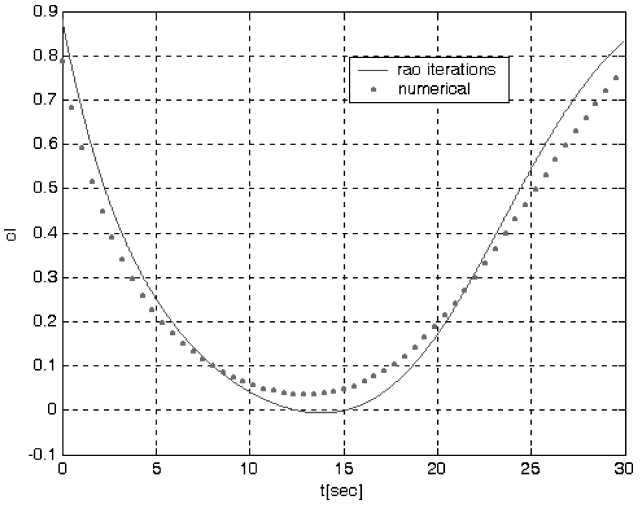

Fig. 14 Control vs time for initial velocity of 800 ft/s.

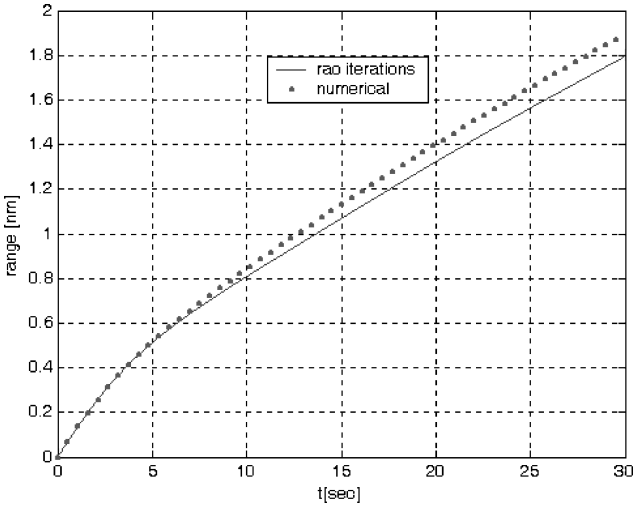

Fig. 15 Range vs time for initial velocity of 800 ft/s.

The initial boundary layer results for $v_0 = 300$ ft/s are shown in Figs. 1–5, for $v_0 = 500$ ft/s in Figs. 6–10, and for $v_0 = 800$ ft/s in Figs. 11–15.

Conclusions

The dichotomic method together with the chosen timescale separation succeeded in creating a good solution to the range optimization problem with a little numerical effort. Three trajectories were

presented. All of the approximated trajectories are pretty close to the exact numerical ones, but it seems that the matching is better for lower initial velocities. For initial velocity of 300 ft/s, all of the approximated state variables and the control are almost identical to the exact variables. For initial velocity of 500 ft/s, all of the approximated state variables and the control are very close to the exact variables, but are not identical, and for initial velocity of 800 ft/s, all of the approximated state variables and the control are in quite good agreement with the exact variables in the first 10 s, and deviate reasonably later on. It is not clear at this point if this tendency is related to the validity of the chosen timescale separation, or to a better convergence of the iteration process for low velocities.

Appendix A: Outer Solution

The outer solution is derived by substituting $\varepsilon = 0$ into the general formalism. Thus, the state equations of the slow variables x and h [Eqs. (2a) and (2b)] and their initial and final values Eqs. (6a) and (6b) remain unchanged. However, the fast variables v and γ stop acting as states and become controls. The left-hand side (LHS) of their state equations (2c) and (2d) is replaced by zero, causing the drag and lift to become functions of γ and the lift coefficient cl to depend on γ and $q\{cl = [w \cdot \cos(\gamma)]/(s \cdot q)\}$.

The cost function remains unchanged, and the Hamiltonian degenerates into

$$H = H^0 = \lambda_x \cdot v \cdot \cos(\gamma) + \lambda_h \cdot v \cdot \sin(\gamma) \tag{A1}$$

The right-hand side of costate equation (5b) becomes zero (because the Hamiltonian is not a function of h any more), and the LHS of Eqs. (5c), and (5d) also become zero (because ε is zero), which complies with the necessary optimal condition for the controls v and γ:

$$\frac{\mathrm{d}\lambda_h}{\mathrm{d}t} = -\frac{\partial H}{\partial h} = 0 \tag{A2}$$

$$\frac{\partial H}{\partial v} = [\lambda_x \cdot \cos(\gamma) + \lambda_h \cdot \sin(\gamma)] = 0 \tag{A3}$$

$$\frac{\partial H}{\partial \gamma} = [-\lambda_x \cdot v \cdot \sin(\gamma) + \lambda_h \cdot v \cdot \cos(\gamma)] = 0 \tag{A4}$$

Appendix B: Zeroth-Order Inner Formalism

The control cl from Eq. (B11) can be substituted in the Hamiltonian from Eq. (B6) to yield the Hamiltonian as function of the state and costate vectors:

Table B1 Inner zeroth formalism ($\tau = t/\varepsilon$)

Equation	Equations	Initial values	Final values
	State equations		
(B1)	$\frac{\mathrm{d}x^i}{\mathrm{d}\tau} = \varepsilon \cdot v^i \cdot \cos(\gamma^i) \underset{\varepsilon=0}{=} 0$	x_0	
(B2)	$\frac{\mathrm{d}h}{\mathrm{d}\tau} = \varepsilon \cdot v \cdot \sin(\gamma) \underset{\varepsilon=0}{=} 0$	h_0	
(B3)	$\frac{\mathrm{d}v^i}{\mathrm{d}\tau} = -\frac{D^i}{m} - g \cdot \sin(\gamma^i)$	v_0	v_0^o
(B4)	$\frac{\mathrm{d}\gamma^i}{\mathrm{d}\tau} = \left(\frac{L^i}{w} - \cos(\gamma^i)\right) \cdot \frac{g}{v^i}$	γ_0	γ^o
(B5)	Cost function redefined to compensate for freezing the slow variables x and h		
	$J = \lim_{\tau_f \to \infty} \int_0^{\tau_f} H^0\left[\lambda_x, \lambda_h, v^i(\tau), \gamma^i(\tau)\right] \mathrm{d}\tau$		
(B6)	$H^i = \lambda_{x_0} \cdot v^i \cdot \cos(\gamma^i) + \lambda_{h_0} \cdot v^i \cdot \sin(\gamma^i) + \lambda_v^i \cdot \left[-\frac{D\left(h_0, v^i, \gamma^i, cl^i\right)}{m} - g \cdot \sin(\gamma^i)\right]$		
	$+ \lambda_\gamma^i \cdot \left[\frac{L}{w}\left(h_0, v^i, \gamma^i, cl^i\right) - \cos(\gamma^i)\right] \cdot \frac{g}{v^i} = 0$		
	Costate equations		
(B7)	$\lambda_x = -1$		
(B8)	$\lambda_h = -\frac{1}{2\sqrt{cd_0 \cdot k}}$		
(B9)	$\frac{\mathrm{d}\lambda_v^i}{\mathrm{d}\tau} = -\frac{\partial H^i}{\partial v^i} = -\left\{\lambda_x \cdot \cos(\gamma^i) + \lambda_h \cdot \sin(\gamma^i) - \frac{\lambda_v^i}{m} \cdot \frac{\partial D}{\partial v^i} + \lambda_\gamma^i \cdot \frac{\partial}{\partial v^i}\left[\frac{L}{w} - \cos(\gamma)\right] \cdot \frac{g}{v^i}\right\}$		
	$= -\left[\lambda_x \cdot \cos(\gamma^i) + \lambda_h \cdot \sin(\gamma^i)\right] + \lambda_v^i \cdot \frac{cd_0 \cdot s}{m} \cdot \frac{\partial q}{\partial v^i} + \lambda_v^i \cdot \frac{k \cdot cl^2 \cdot s}{m} \cdot \frac{\partial q}{\partial v^i}$		
	$- \lambda_\gamma^i \cdot \frac{0.5 \cdot \rho(h_0) \cdot cl \cdot s}{m} - \lambda_\gamma^i \cdot \frac{g \cdot \cos(\gamma^i)}{v^{i2}}$		
	$= \lambda_\gamma^i \underset{(B11)}{=} 2 \cdot k \cdot cl^i \cdot v^i \cdot \lambda_v^i \Rightarrow cl^i = \frac{\lambda_\gamma^i}{2 \cdot k \cdot v^i \cdot \lambda_v^i}; \qquad \frac{\partial q^i}{\partial v^i} = \frac{\partial\left(0.5 \cdot \rho(h_0) \cdot v^{i2}\right)}{\partial v^i} = \rho(h_0) \cdot v$		
	$\because \frac{\mathrm{d}\lambda_v^i}{\mathrm{d}\tau} = -\left[\lambda_x \cdot \cos(\gamma) + \lambda_h \cdot \sin(\gamma)\right] + \left[\frac{cd_0 \cdot \rho(h_0) \cdot s}{m}\right] \cdot \lambda_v^i \cdot v - g \cdot \cos(\gamma) \cdot \frac{\lambda_\gamma^i}{v^2}$		
(B10)	$H^i(\gamma^i) = \lambda_X \cdot v^i \cdot \cos(\gamma^i) + \lambda_h \cdot v^i \cdot \sin(\gamma^i) - \lambda_v^i \cdot g \cdot \sin(\gamma^i) - \lambda_\gamma^i \cdot \cos(\gamma^i) \cdot \frac{g}{v^i}$		
	$\dot{\lambda}_\gamma = -\frac{\partial H^i}{\partial \gamma^i} = -\left[-\lambda_X \cdot v^i \cdot \sin(\gamma^i) + \lambda_h \cdot v^i \cdot \cos(\gamma^i) - \lambda_v^i \cdot g \cdot \cos(\gamma^i) + \lambda_\gamma^i \cdot \sin(\gamma^i) \cdot \frac{g}{v^i}\right]$		
	$= \lambda_X \cdot v^i \cdot \sin(\gamma^i) - \lambda_h \cdot v^i \cdot \cos(\gamma^i) + \lambda_v^i \cdot g \cdot \cos(\gamma^i) - \lambda_\gamma^i \cdot \sin(\gamma^i) \cdot \frac{g}{v^i}$		
(B11)	$\lambda_\gamma^i = 2 \cdot k \cdot cl^i \cdot v^i \cdot \lambda_v^i$		

$$H^i = \lambda_X \cdot v^i \cdot \cos(\gamma^i) + \lambda_h \cdot v^i \cdot \sin(\gamma^i) - \lambda_v \cdot \frac{cd_0 \cdot \rho(h_0)}{2 \cdot m} \cdot v^{i^2} \cdot s + \frac{\lambda_\gamma^{i^2} \cdot \rho(h_0)}{8 \cdot k \cdot m \cdot \lambda_v^i} \cdot s - \lambda_v^i \cdot g \cdot \sin(\gamma^i) - \lambda_\gamma^i \cdot \cos(\gamma^i) \cdot \frac{g}{v^i} \quad \text{(B12)}$$

Appendix C: Hamiltonian First-Order Partial Derivatives in the Initial Layer

The partial derivatives of H^i with respect to the state components v^i and γ^i and the Lagrange coefficients λ_v^i and λ_γ^i are derived from Eq. (B12),

$$H_v^i = \lambda_X \cdot \cos(\gamma^i) + \lambda_h \cdot \sin(\gamma^i) - \lambda_v^i \cdot [cd_0 \cdot \rho(h_0)]/m \cdot v \cdot s + \lambda_\gamma^i \cdot \cos(\gamma^i) \cdot g \Big/ v^{i^2}$$

$$H_{vv}^i = -\lambda_v^i \cdot [cd_0 \cdot \rho(h_0)]/m \cdot s - 2 \cdot \lambda_\gamma^i \cdot \cos(\gamma^i) \cdot g \Big/ v^{i^3}$$

$$H_{v\gamma}^i = -\lambda_X \cdot \sin(\gamma^i) + \lambda_h \cdot \cos(\gamma^i) - \lambda_\gamma \cdot \sin(\gamma^i) \cdot g \Big/ v^{i^2}$$

$$H_\gamma^i = -\lambda_X \cdot v^i \cdot \sin(\gamma^i) + \lambda_h \cdot v^i \cdot \cos(\gamma^i) - \lambda_v \cdot g \cdot \cos(\gamma^i) + \lambda_\gamma \cdot \sin(\gamma^i) \cdot g/v^i$$

$$H_{\gamma\gamma}^i = -\lambda_X \cdot v^i \cdot \cos(\gamma^i) - \lambda_h \cdot v^i \cdot \sin(\gamma^i) + \lambda_v^i \cdot g \cdot \sin(\gamma^i) + \lambda_\gamma^i \cdot \cos(\gamma) \cdot g/v^i$$

$$H_{\gamma v}^i = -\lambda_X \cdot \sin(\gamma^i) + \lambda_h \cdot \cos(\gamma^i) - \lambda_\gamma^i \cdot \sin(\gamma^i) \cdot g \Big/ v^{i^2}$$

Appendix D: Hamiltonian Second-Order Partial Derivatives in the Initial Layer

The partial derivatives in vector and matrix form can be obtained from Appendix C,

$$H_\lambda^i = \begin{bmatrix} H_{\lambda_v}^i \\ H_{\lambda_\gamma}^i \end{bmatrix} = \begin{bmatrix} \left[-\frac{cd_0 \cdot \rho(h_0) \cdot s}{2 \cdot m}\right] \cdot v^{i^2} - \left[\frac{\rho(h_0) \cdot s}{8 \cdot k \cdot m}\right] \cdot \frac{\lambda_\gamma^{i^2}}{\lambda_v^{i^2}} - g \cdot \sin(\gamma^i) \\ \left[\frac{\rho(h_0) \cdot s}{4 \cdot k \cdot m}\right] \cdot \frac{\lambda_\gamma^i}{\lambda_v^i} - g \cdot \frac{\cos(\gamma^i)}{v^i} \end{bmatrix}$$

$$H_x^i = \begin{bmatrix} H_v^i \\ H_\gamma^i \end{bmatrix} = \begin{bmatrix} \lambda_X \cdot \cos(\gamma^i) + \lambda_h \cdot \sin(\gamma^i) - \lambda_v^i \cdot \frac{cd_0 \cdot \rho(h_0)}{m} \cdot v^i \cdot s + \lambda_\gamma^i \cdot \cos(\gamma^i) \cdot \frac{g}{v^{i^2}} \\ -\lambda_X \cdot v^i \cdot \sin(\gamma^i) + \lambda_h \cdot v^i \cdot \cos(\gamma^i) - \lambda_v^i \cdot g \cdot \cos(\gamma^i) + \lambda_\gamma^i \cdot \sin(\gamma^i) \cdot \frac{g}{v^i} \end{bmatrix}$$

$$H_{\lambda\lambda}^i = \begin{bmatrix} H_{\lambda_v\lambda_v}^i & H_{\lambda_v\lambda_\gamma}^i \\ H_{\lambda_v\lambda_\gamma}^i & H_{\lambda_\gamma\lambda_\gamma}^i \end{bmatrix} = \left[\frac{\rho(h_0) \cdot s}{4 \cdot k \cdot m}\right] \cdot \begin{bmatrix} \frac{\lambda_\gamma^{i^2}}{\lambda_v^{i^3}} & -\frac{\lambda_\gamma^i}{\lambda_v^{i^2}} \\ -\frac{\lambda_\gamma^i}{\lambda_v^{i^2}} & \frac{1}{\lambda_v^i} \end{bmatrix} \quad H_{\lambda x}^i = \begin{bmatrix} H_{\lambda_v v}^i & H_{\lambda_v \gamma}^i \\ H_{\lambda_\gamma v}^i & H_{\lambda_\gamma \gamma}^i \end{bmatrix} = \begin{bmatrix} \left[-\frac{cd_0 \cdot \rho(h_0) \cdot s}{m}\right] \cdot v^i & -g \cdot \cos(\gamma^i) \\ g \cdot \frac{\cos(\gamma^i)}{v^{i^2}} & g \cdot \frac{\sin(\gamma^i)}{v^i} \end{bmatrix}$$

$$H_{x\lambda}^i = \left[H_{\lambda x}^i\right]^T$$

$$H_{xx}^i = \begin{bmatrix} H_{vv}^i & H_{v\gamma}^i \\ H_{\gamma v}^i & H_{\gamma\gamma}^i \end{bmatrix} = \begin{bmatrix} -\left[\frac{cd_0 \cdot \rho(h_0) \cdot s}{m}\right] \cdot \lambda_v^i - 2 \cdot \lambda_\gamma^i \cdot \cos(\gamma^i) \cdot \frac{g}{v^{i^3}} & \left[-\lambda_X \cdot \sin(\gamma) + \lambda_h \cdot \cos(\gamma) - \lambda_\gamma^i \cdot \sin(\gamma) \cdot \frac{g}{v^{i^2}}\right] \\ \left[-\lambda_X \cdot \sin(\gamma^i) + \lambda_h \cdot \cos(\gamma^i) - \lambda_\gamma^i \cdot \sin(\gamma^i) \cdot \frac{g}{v^{i^2}}\right] & \left[-\lambda_X \cdot v^i \cdot \cos(\gamma^i) - \lambda_h \cdot v \cdot \sin(\gamma^i) + \lambda_v^i \cdot g \cdot \sin(\gamma) + \lambda_\gamma^i \cdot \cos(\gamma) \cdot \frac{g}{v^i}\right] \end{bmatrix}$$

Appendix E: Riccati Matrix P in Steady State

The matrix

$$\dot{P} = -P H_{\lambda x} - H_{x\lambda} P - P H_{\lambda\lambda} P - H_{xx}$$

$$P = \begin{pmatrix} P_{11} & P_{12} \\ P_{21} & P_{22} \end{pmatrix}$$

In steady state,

$$0 = -\bar{P} \bar{H}_{\lambda x} - \bar{H}_{x\lambda} \bar{P} - \bar{P} \bar{H}_{\lambda\lambda} \bar{P} - \bar{H}_{xx}, \qquad \bar{P} = \begin{pmatrix} \bar{P}_{11} & \bar{P}_{12} \\ \bar{P}_{21} & \bar{P}_{22} \end{pmatrix}$$

The last equation is an algebraic one and can be solved analytically to yield:

$$\bar{P}_{11} = \frac{1}{g} \cdot \left\{ -\frac{1}{2 \cdot \sqrt{cd_0 \cdot k}} - \frac{12 \cdot \sqrt{cd_0 \cdot k}}{(1 + 4 \cdot cd_0 \cdot k)} + 4 \frac{\sqrt{(1 + 13 \cdot cd_0 \cdot k)}}{(1 + 4 \cdot cd_0 \cdot k)} \right\}$$

$$\bar{P}_{12} = \frac{\bar{v}}{g} \cdot \left\{ \frac{-2 \cdot (1 + 16 \cdot cd_0 \cdot k) + 8 \cdot \sqrt{cd_0 \cdot k} \cdot \sqrt{(1 + 13 \cdot cd_0 \cdot k)}}{(1 + 4 \cdot cd_0 \cdot k)} \right\}$$

$$\bar{P}_{22} = \frac{\bar{v}^2}{g} \cdot \left\{ \left[\frac{-(1 + 16 \cdot cd_0 \cdot k) + 4 \cdot \sqrt{cd_0 \cdot k} \cdot \sqrt{(1 + 13 \cdot cd_0 \cdot k)}}{(1 + 4 \cdot cd_0 \cdot k)} \right] \cdot \left[\frac{1 + 12 \cdot cd_0 \cdot k}{2 \cdot \sqrt{cd_0 \cdot k}} \right] + 2 \cdot \sqrt{cd_0 \cdot k} + \frac{1}{2 \cdot \sqrt{cd_0 \cdot k}} \right\}$$

The velocity at steady state is defined in Eq. (8b) as

$$\bar{v}^2 \equiv v_0^{o^2} = 2/\rho(h_0)\cdot(w/s)\sqrt{k/cd_0}\cdot 1\Big/\sqrt{1+4\cdot cd_0\cdot k}$$

Appendix F: Calculation of λ at $t=0$

All of the variables here refer to the inner layer, but the upper label is omitted. From Appendix D,

$$H_\lambda = \begin{bmatrix} H_{\lambda_v} \\ H_{\lambda_\gamma} \end{bmatrix} = \begin{bmatrix} \left[-\frac{cd_0\cdot\rho(h_0)\cdot s}{2\cdot m}\right]\cdot v^2 - \left[\frac{\rho(h_0)\cdot s}{8\cdot k\cdot m}\right]\cdot\frac{\lambda_\gamma^2}{\lambda_v^2} - g\cdot\sin(\gamma) \\ \left[\frac{\rho(h_0)\cdot s}{4\cdot k\cdot m}\right]\cdot\frac{\lambda_\gamma}{\lambda_v} - g\cdot\frac{\cos(\gamma)}{v} \end{bmatrix} = \begin{bmatrix} A - B\cdot\frac{\lambda_\gamma^2}{\lambda_v^2} \\ C + 2B\cdot\frac{\lambda_\gamma}{\lambda_v} \end{bmatrix} \tag{F1}$$

$$A \equiv \left[-\frac{cd_0\cdot\rho(h_0)\cdot s}{2\cdot m}\right]\cdot v^2 - g\cdot\sin(\gamma) \tag{F2}$$

$$B \equiv \left[\frac{\rho(h_0)\cdot s}{8\cdot k\cdot m}\right] \tag{F3}$$

$$C \equiv -g\cdot\frac{\cos(\gamma)}{v} \tag{F4}$$

$$H_x = \begin{bmatrix} H_v \\ H_\gamma \end{bmatrix} = \begin{bmatrix} \lambda_X\cdot\cos(\gamma) + \lambda_h\cdot\sin(\gamma) - \lambda_v\cdot\frac{cd_0\cdot\rho(h_0)}{m}\cdot v\cdot s + \lambda_\gamma\cdot\cos(\gamma)\cdot\frac{g}{v^2} \\ -\lambda_X\cdot v\cdot\sin(\gamma) + \lambda_h\cdot v\cdot\cos(\gamma) - \lambda_v\cdot g\cdot\cos(\gamma) + \lambda_\gamma\cdot\sin(\gamma)\cdot\frac{g}{v} \end{bmatrix} = \begin{bmatrix} D - E\cdot\lambda_v + F\cdot\lambda_\gamma \\ G - J\cdot\lambda_v + K\cdot\lambda_\gamma \end{bmatrix} \tag{F5}$$

$$D \equiv \lambda_X\cdot\cos(\gamma) + \lambda_h\cdot\sin(\gamma) \tag{F6}$$

$$E \equiv \frac{cd_0\cdot\rho(h_0)}{m}\cdot v\cdot s \tag{F7}$$

$$F \equiv \cos(\gamma)\cdot\frac{g}{v^2} \tag{F8}$$

$$G \equiv -\lambda_X\cdot v\cdot\sin(\gamma) + \lambda_h\cdot v\cdot\cos(\gamma) \tag{F9}$$

$$J \equiv g\cdot\cos(\gamma) \tag{F10}$$

$$K \equiv \sin(\gamma)\cdot\frac{g}{v} \tag{F11}$$

From Eq. (22),

$$[-P(0)I]\cdot\begin{bmatrix} H_\lambda(0) \\ -H_x(0) \end{bmatrix} = \begin{bmatrix} 0 \\ 0 \end{bmatrix} \tag{F12}$$

$$P = \begin{pmatrix} P_{11} & P_{12} \\ P_{21} & P_{22} \end{pmatrix} \tag{F13}$$

$$-P_{11}(0)\cdot H_{\lambda_v}(0) - P_{12}(0)\cdot H_{\lambda_\gamma}(0) - H_v(0) = 0 \tag{F14}$$

$$-P_{21}(0)\cdot H_{\lambda_v}(0) - P_{22}(0)\cdot H_{\lambda_\gamma}(0) - H_\gamma(0) = 0 \tag{F15}$$

or

$$P_{11}(0)\cdot H_{\lambda_v}(0) + P_{12}(0)\cdot H_{\lambda_\gamma}(0) + H_v(0) = 0 \tag{F16}$$

$$P_{21}(0)\cdot H_{\lambda_v}(0) + P_{22}(0)\cdot H_{\lambda_\gamma}(0) + H_\gamma(0) = 0 \tag{F17}$$

$$P_{11}(0)\cdot\left[A(0) - B\cdot\lambda_\gamma^2\Big/\lambda_v^2\right] + P_{12}(0)\cdot[C(0) + 2B\cdot\lambda_\gamma/\lambda_v] + D(0) - E(0)\cdot\lambda_v + F(0)\cdot\lambda_\gamma = 0 \tag{F18}$$

$$P_{21}(0)\cdot\left[A(0) - B\cdot\lambda_\gamma^2\Big/\lambda_v^2\right] + P_{22}(0)\cdot[C(0) + 2B\cdot\lambda_\gamma/\lambda_v] + G(0) - J(0)\cdot\lambda_v + K(0)\cdot\lambda_\gamma = 0 \tag{F19}$$

or

$$c_1\cdot\lambda_\gamma^2\Big/\lambda_v^2 + c_2\cdot\lambda_\gamma/\lambda_v + c_3\cdot\lambda_v + c_4\cdot\lambda_\gamma + c_5 = 0 \tag{F20}$$

$$c_6\cdot\lambda_\gamma^2\Big/\lambda_v^2 + c_7\cdot\lambda_\gamma/\lambda_v + c_8\cdot\lambda_v + c_9\cdot\lambda_\gamma + c_{10} = 0$$

$$c_1 = -P_{11}(0)\cdot B, \qquad c_2 = 2\cdot P_{12}(0)\cdot B, \qquad c_3 = -E(0)$$

$$c_4 = F(0), \qquad c_5 = P_{11}(0)\cdot A(0) + P_{12}(0)\cdot C(0) + D(0) \tag{F21}$$

$$c_6 = -P_{21}(0)\cdot B, \qquad c_7 = 2\cdot P_{22}(0)\cdot B, \qquad c_8 = -J(0)$$

$$c_9 = K(0), \qquad c_{10} = P_{21}(0)\cdot A(0) + P_{22}(0)\cdot C(0) + G(0) \tag{F22}$$

$$x \triangleq \lambda_v(0) \tag{F23}$$

$$y \triangleq \lambda_\gamma(0)/\lambda_v(0) \tag{F24}$$

$$c_1\cdot y^2 + c_2\cdot y + c_3\cdot x + c_4\cdot x\cdot y + c_5 = 0 \tag{F25}$$

$$c_6\cdot y^2 + c_7\cdot y + c_8\cdot x + c_9\cdot x\cdot y + c_{10} = 0 \tag{F26}$$

$$x\cdot(c_8 + c_9\cdot y) = -c_6\cdot y^2 - c_7\cdot y - c_{10} \tag{F27}$$

$$x = \frac{-c_6\cdot y^2 - c_7\cdot y - c_{10}}{c_8 + c_9\cdot y}, \qquad c_8 + c_9\cdot y \neq 0$$

$$c_1\cdot y^2 + c_2\cdot y - c_3\cdot\left[\frac{c_6\cdot y^2 + c_7\cdot y + c_{10}}{c_8 + c_9\cdot y}\right] - c_4\cdot\left[\frac{c_6\cdot y^2 + c_7\cdot y + c_{10}}{c_8 + c_9\cdot y}\right]\cdot y + c_5 = 0 \tag{F28}$$

$$c_1\cdot y^2\cdot(c_8 + c_9\cdot y) + c_2\cdot y\cdot(c_8 + c_9\cdot y) - c_3\cdot\left(c_6\cdot y^2 + c_7\cdot y + c_{10}\right) - c_4\cdot\left(c_6\cdot y^2 + c_7\cdot y + c_{10}\right)\cdot y + c_5\cdot(c_8 + c_9\cdot y) = 0 \tag{F29}$$

$$y^3\cdot(c_1\cdot c_9 - c_4\cdot c_6) + y^2\cdot(c_1\cdot c_8 + c_2\cdot c_9 - c_3\cdot c_6 - c_4\cdot c_7) + y\cdot(c_2\cdot c_8 - c_3\cdot c_7 - c_4\cdot c_{10} + c_5\cdot c_9) - c_3\cdot c_{10} + c_5\cdot c_8 = 0 \tag{F30}$$

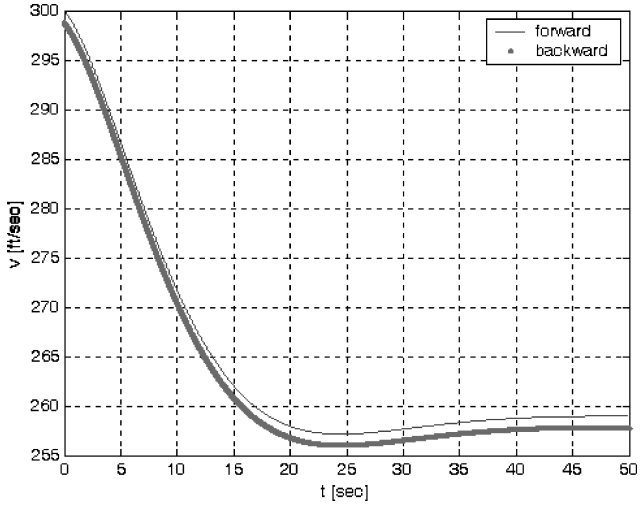

Fig. G1 Velocity profile for initial velocity of 300 ft/s.

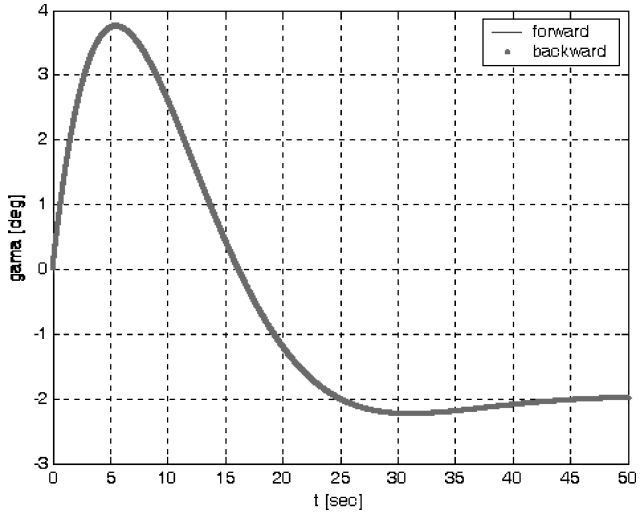

Fig. G2 Path-angle profile for initial velocity of 300 ft/s.

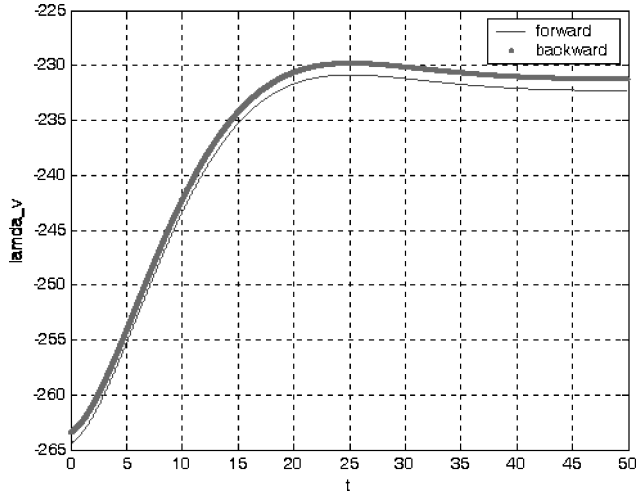

Fig. G3 Lagrange multiplier λ_v profile for initial velocity of 300 ft/s.

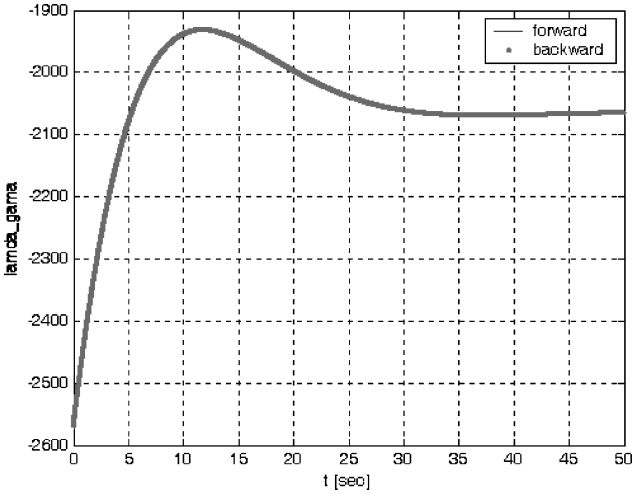

Fig. G4 Lagrange multiplier λ_γ profile for initial velocity of 300 ft/s.

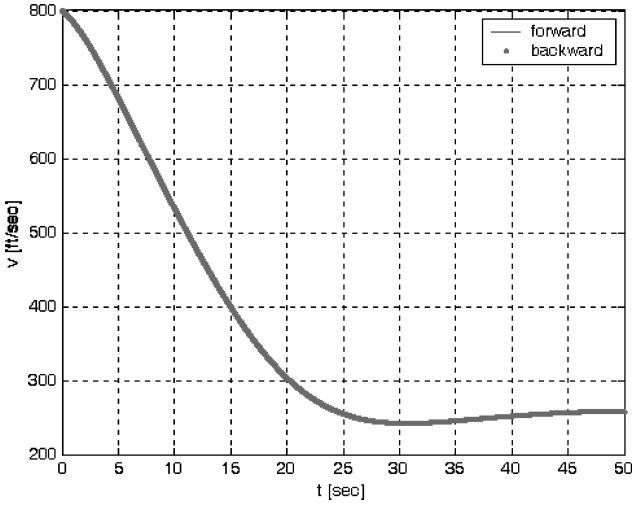

Fig. G5 Velocity profile for initial velocity of 800 ft/s.

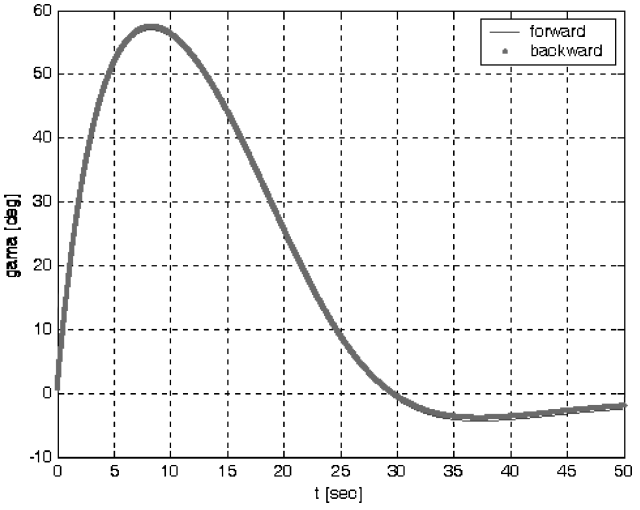

Fig. G6 Path-angle profile for initial velocity of 800 ft/s.

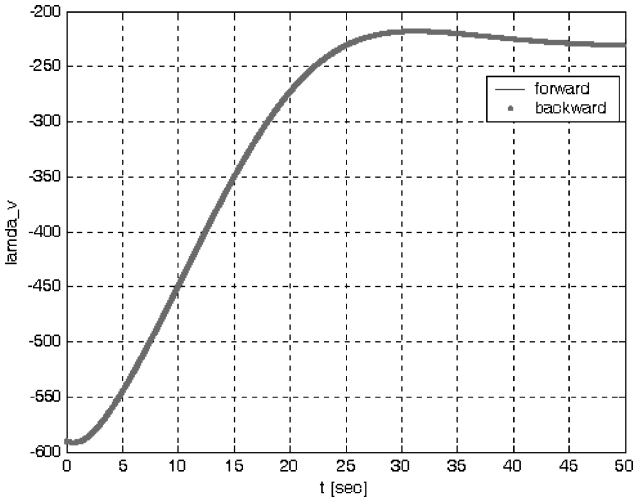

Fig. G7 Lagrange multiplier λ_v profile for initial velocity of 800 ft/s.

$$r_1 = c_1 \cdot c_9 - c_4 \cdot c_6, \qquad r_2 = c_1 \cdot c_8 + c_2 \cdot c_9 - c_3 \cdot c_6 - c_4 \cdot c_7$$

$$r_3 = c_2 \cdot c_8 - c_3 \cdot c_7 - c_4 \cdot c_{10} + c_5 \cdot c_9, \qquad r_4 = -c_3 \cdot c_{10} + c_5 \cdot c_8$$

$$y^3 \cdot r_1 + y^2 \cdot r_2 + y \cdot r_3 + r_4 = 0 \tag{F31}$$

The coefficients $(r_1, \ldots, r_4)$ are functions of the initial state (h_0, v_0, γ_0) and the system different constants. This equation has an analytical solution, and once y is derived, then $\lambda_v(0)$ can be calculated from Eq. (F28) and then $\lambda_\gamma(0)$ can be derived from y and $\lambda_v(0)$,

$$\lambda_\gamma(0) = y \cdot \lambda_v(0) \tag{F32}$$

Appendix G: Convergence Results

Figures G1–G8 show the last step of the iteration process for two initial velocities of 300 and 800 ft/s.

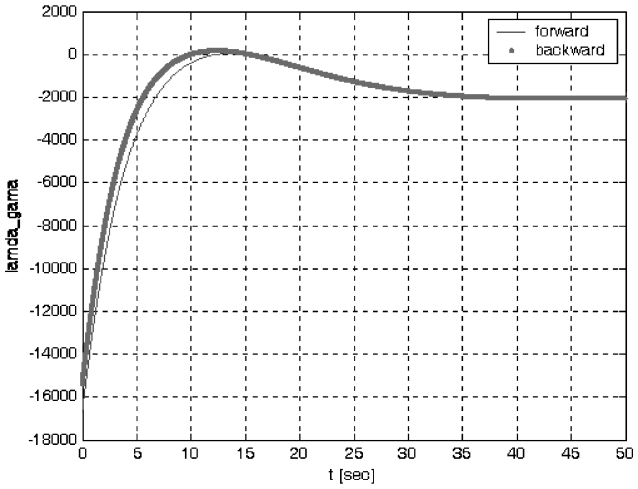

Fig. G8 Lagrange multiplier λ_γ profile for initial velocity of 800 ft/s.

References

[1]Rao, A. V., "Riccati Dichotomic Basis Method for Solving Hypersensitive Optimal Control Problems," *Journal of Guidance, Control, and Dynamics*, Vol. 26, No. 1, pp. 185–189.

[2]Rao, A. V., and Mease, K. D., "Dichotomic Basis Approach to Solving Hyper-Sensitive Optimal Control Problems," *Automatica*, Vol. 35, No. 4, 1999, pp. 633–642.

[3]Rao, A. V., and Mease, K. D., "Eigenvector Approximate Dichotomic Basis Method for Solving Hyper-Sensitive Optimal Control Problems," *Optimal Control Applications and Methods*, Vol. 21, No. 1, 2000, pp. 1–19.

[4]Ardema, M. D., and Rajan, N., "Separation of Time Scales in Aircraft Trajectory Optimization," *Journal of Guidance, Control, and Dynamics*, Vol. 8, No. 2, 1985, pp. 275–278.

[5]Shapira, I., and Ben-Asher, J. Z., "Singular Perturbation Analysis of Optimal Glide," *Proceeding of the AIAA/AFM Conference*, Aug. 2002.

[6]Shapira, I., and Ben-Asher, J. Z., "Singular Perturbation Analysis of Optimal Glide," *Journal of Guidance, Control, and Dynamics*, Vol. 27, No. 5, 2004, pp. 915–918.